Chapter 5
Fundamentals of Network Densification

Abhishek K. Gupta, Nithin V. Sabu, and Harpreet S. Dhillon

5.1 Introduction to Densification

With applications in all sectors of human activity, wireless communications is widely regarded as one of the most pervasive technology enablers on the planet. Starting with Marconi's first transatlantic transmission in 1899 to the introduction of worldwide cellular networks in the 1980s and their subsequent evolution from supporting predominantly voice-driven applications to a largely data-driven services, the past 120 years has seen a remarkable transformation of this technology. More recent advancements in Internet-enabled computing and communication devices, primarily smartphones, tablets, wearables, and laptops, have increased mobile data traffic tremendously. According to the well-known predictions by Cisco [1], there has been almost 4000-fold growth in the mobile data traffic over the past 10 years and nearly 400-million-fold growth over the past 15 years. The monthly global mobile data traffic is estimated to be well over 35 exabytes already [2]. Developing efficient techniques to cope up with this data deluge is a key challenge faced by the wireless communications industry today.

A. Gupta gratefully acknowledges the support of the Science and Engineering Research Board (DST, India) under the grant SRG/2019/001459.

H. S. Dhillon gratefully acknowledges the support of the US National Science Foundation (Grant CNS-1617896)

A. K. Gupta · N. V. Sabu
Department of Electrical Engineering, Indian Institute of Technology, Kanpur, Uttar Pradesh, India
e-mail: gkrabhi@iitk.ac.in; nithinvs@iitk.ac.in

H. S. Dhillon (✉)
Wireless@VT, Department of ECE, Virginia Tech, Blacksburg, VA, USA
e-mail: hdhillon@vt.edu

X. Lin, N. Lee (eds.), *5G and Beyond*, https://doi.org/10.1007/978-3-030-58197-8_5

Since history is the best teacher, it will be instructive to understand which technologies have contributed the most to the increase in wireless network capacity in the past. For this, we rely on the well-known observations made by Martin Cooper, Chairman Emeritus of ArrayComm, that for the past 104 years, the number of *conversations* (voice or data) that can be carried out in a given area using all the available radio spectrum has doubled every 2.5 years [3]. This observation is often termed *Cooper's law*. That means there has been a one million fold increase in "capacity" over the past 45 years. Out of this one million fold increase, almost 1600 times increase is attributed to spectrum reuse (equivalently, *denser* deployments), 25 times to more spectrum, 5 times to modulation and coding, and 5 times to frequency division. This fact alone should be sufficient to put the importance of network densification in perspective.

The performance of a wireless system is primarily measured in terms of the achievable data rate, which is further linked to three important metrics, namely, available spectrum, link efficiency, and signal to interference plus noise ratio (SINR), via the famous Shannon-Hartley theorem. Specifically, the throughput of a single user in a cellular network can be expressed as [4]

$$c = m\left(\frac{W}{n}\right)\log_2\left(1+\mathrm{SINR}\right), \tag{5.1}$$

where W denotes the signal bandwidth of the base station (BS), n denotes the number of user equipment (UE) associated with this BS (that are sharing the same bandwidth), and hence W/n is the bandwidth available to each UE. Further, m captures the increase in capacity because of having multiple antennas, e.g., through supporting simultaneous streams of information. Assuming the densities of BSs and UEs (equivalently, average number of nodes per unit area) be λ, and λ_u, respectively, n would be of the order of λ_u/λ. From the above discussion, it is evident that the UE throughput can be increased by increasing either or all of the four parameters: m, W, SINR, or λ. Here, W can be increased by allocating more spectrum, m can be increased by adding more antennas at the BS and UE, and λ can be increased by adding more BSs, which is also known as *densification* and is the main topic of this chapter. As noted above already, densification alone has contributed almost 1600-fold increase out of the total one million fold increase in capacity over the past 45 years. This is primarily because the addition of more BSs offloads users from the existing BSs, thus providing higher resources to each user, which is often termed the *cell splitting gain* [5].

Early cellular networks were sparse, and hence densification of these networks helped them fill coverage holes by increasing the received serving power at UEs. These BSs providing service to large areas (equivalently, having large coverage footprints) are called macrocell BSs. In the case of third-generation (3G) cellular systems, the primary aim of macro BS densification was to increase the transmission rate in specific areas, for example, macro-BSs deployed in the urban areas [6]. An effect of increased interference due to the densification of BSs was mitigated using frequency reuse and sectorized BS technologies. The density of macro-BSs for 3G

cellular systems was not more than 4–5 BSs/km^2. In the fourth-generation (4G) cellular networks, including long-term evolution-advanced (LTE-A), new types of BSs, such as micro-cells, pico-cells, and femto-cells, have been deployed for enabling high-speed data transmission. The targeted density of these new BSs, often collectively called small cells, is about 8–10 BSs/km^2 [6]. The micro-cells and pico-cells are often deployed by service providers to complement the capacity of the existing networks, e.g., to enhance the throughput in specific areas in order to provide in-store services such as in malls and stadiums. On the other hand, femtocells are deployed directly by the users to improve coverage or capacity in small areas, such as in a house or in office. In both 3G and 4G cellular systems, the aim of BS densification was to improve the transmission rate, and the major challenge was interference mitigation. The Third Generation Partnership Project (3GPP) 4G LTE networks included small cell technology in their specifications throughout the second decade of 2000 up to now [7]. Over 14 million small cell BSs have been deployed worldwide till February 2016, and out of this over 12 million BSs were residential.

Now coming to the fifth-generation (5G) cellular networks, the key technologies of 5G are massive multiple-input multiple-output (MIMO) antennas, millimeter wave communications, and small cells. In massive MIMO, hundreds of antennas are used for transmitting gigabit-level data traffic. If we constrain the 5G BS power to about the same as that of 4G BS power, there will be a 10–20-fold reduction in transmission power per antenna compared to 4G BS power. As a result of this, the radius of the cell has to be reduced. Systems will also tend to use millimeter-wave frequencies owing to the availability of hundreds of megahertz bandwidth in these bands. Given the blockage sensitivity of these frequencies, the transmission range in such cases would be limited to about 100 m or so [6]. Therefore, it is expected that 5G networks would consist of small cells deployed at a very high density. Despite that, the interference in these bands remains low and spatially sparse because of highly directional transmission. This opens up the opportunities to deploy various types of services all sharing the same band, thus improving spectrum utilization [8].

With this background, we now revisit (5.1) to express the total throughout per unit area (also termed area spectrum efficiency) as

$$R \approx \lambda_{\mathrm{u}} m \left(\frac{W}{\lambda_{\mathrm{u}}/\lambda} \right) \log_2 (1 + \mathrm{SINR}) \propto \lambda. \tag{5.2}$$

This essentially means that assuming other parameters are not affected with an increase in λ (an assumption that will be scrutinized in the sequel), densification can lead to linear increase in the throughput. This solution works up to the current density of BSs. However, the question is whether this linear relation would remain valid for infinite densification or whether we have already reached the fundamental limit to the gains that can be achieved by densification [5]. Answering this question comprehensively is the main goal of this chapter.

5.2 General System Model and Performance Metrics

We will start the discussion by describing the general cellular network model adopted in this chapter. We will also identify the key performance metrics using which the performance of a cellular network can be quantitatively measured.

Network model We consider a cellular network with multiple BSs and UEs in which the BSs are located in a 2D space with density λ (i.e., the average number of BSs in the unit area is λ), and the UEs are spread in a stationary manner with density λ_u. The set of BSs is denoted as $\mathcal{N}_B$ and UEs as $\mathcal{N}_U$. Each UE is associated with one BS, which acts as the serving BS for this user, while the rest of the BSs act as interferers. All the calculations in this chapter will require us to study the impact of the network on the performance of a given UE. Without loss of generality, we will focus on the typical UE that will be placed at the origin.

Channel model Consider an individual BS (let us index it to be the ith BS) located at $\mathbf{x}_i$. The transmit power of this BS is p_i. The signal power attenuates according to a function $\ell(\cdot)$ termed path-loss function. The received signal power from this BS at the typical UE is given as

$$p_{ri} = p_i G_i \ell(\|\mathbf{x}_i\|)$$

where G_i is a random variable denoting fading caused by various scatterers and obstacles present in the transmitter-receiver path. The path-loss function $\ell(\cdot)$ plays an important role in determining the average received power and depends on the propagation environment. If the propagation environment is free space, the path-loss function is given as the simple power-law relation

$$\ell(r) = \left(\frac{\lambda_s}{4\pi r}\right)^2 \propto r^{-2},$$

where λ_s is the wavelength of the transmitted signal. The above equation is well-known by the name of Friis transmission equation. While this is conceptually simple to work with, it is not valid for environments where the propagation medium consists of blockages, shadowing effects, multiple signal reflections, and scattering. Therefore, it is desirable to use path-loss models that embody the simplicity of the Friis equation but capture the effect of the aforementioned propagation effects reasonably accurately. A widely accepted and used model is the one in which the distance dependence is generalized to $r^{-\alpha}$, where α is the path-loss exponent. The path-loss, thus, is given as

$$\ell(r) = Cr^{-\alpha}$$

where C is a constant termed near-field gain which represents the path-loss at unit distance. The value of α depends upon the transmission frequency and the

propagation environment and is generally determined empirically. We would refer to this path-loss model as the *standard path-loss model* throughout the chapter. Since this will be extended further in the chapter to a multi-slope model, we will also refer to this as a *single slope path-loss model* wherever necessary.

SINR model Let us denote the BS that serves the typical UE by index 0. Hence, the received power from this BS at the typical UE is denoted by $S = p_{\mathrm{r}0}$. If the UE density is finite, it is possible that some BSs do not have any associated UEs because of which they can suspend their downlink transmission in order to avoid interference to the other UEs. Let $\mathcal{N}_{\mathrm{aB}}$ denote the set of all active BSs. Let the active BS density be λ_{a}, which is essentially equal to the density of the transmitting BSs. If the UE density is infinite, or significantly larger than BS density, or it scales with the BS density as network densifies, all BSs will be considered active, i.e., $\mathcal{N}_{\mathrm{aB}} = \mathcal{N}_{\mathrm{B}}$ all the time. The interference power I at the typical UE is given as

$$I = \sum_{i \neq 0,\ i \in \mathcal{N}_{\mathrm{aB}}} p_{\mathrm{r}i}\,.$$

The signal to noise power ratio (SNR) is the ratio of serving signal power to the noise power, which is given as

$$\mathrm{SNR} = \frac{p_{\mathrm{r}0}}{\sigma^2},$$

where σ^2 is the noise power. Similarly, the SINR at the UE is given as

$$\mathrm{SINR} = \frac{S}{\sigma^2 + I}.$$

In scenarios where thermal noise is negligible compared to the interference power, SIR (signal to interference ratio) is useful to consider, which can be defined as

$$\mathrm{SIR} = \frac{S}{I}.$$

Performance metrics We will consider the following three metrics for evaluating the performance of the cellular network:

1. ***Coverage probability:*** Let γ_{s} be the SINR threshold required at the typical user for successful transmission. The coverage probability of the typical UE is defined as

$$\mathrm{p_c} = \mathbb{P}\left(\mathrm{SINR} > \gamma_{\mathrm{s}}\right), \tag{5.3}$$

   which denotes the probability that the typical UE can achieve the target SINR γ_{s}. Coverage probability can also be thought as the complementary cumulative

distribution function (CCDF) of the SINR. In scenarios where thermal noise is negligible, the coverage probability can also be defined in terms of SIR as

$$\mathrm{p_{cI}} = \mathbb{P}\left(\mathrm{SIR} > \gamma_\mathrm{s}\right). \tag{5.4}$$

2. ***Potential throughput (PT):*** The potential throughput of the cellular network is defined as

$$\tau = \lambda_\mathrm{a} \mathrm{p_c}(\lambda, \alpha) \times \log(1 + \gamma_\mathrm{s}). \tag{5.5}$$

Note that the potential throughput denotes the average number of bits transmitted successfully per unit area. While neglecting thermal noise, the potential throughput is defined as

$$\tau_\mathrm{I} = \lambda_\mathrm{a} \mathrm{p_{cI}}(\lambda, \alpha) \times \log(1 + \gamma_\mathrm{s}). \tag{5.6}$$

3. ***Area spectral efficiency (ASE):*** The ASE of the network is defined as

$$\mathcal{A} = \lambda_\mathrm{a} \mathbb{E}\left[\log(1 + \gamma_\mathrm{s}) \mathbb{1}\left(\mathrm{SINR} > \gamma_\mathrm{s}\right)\right] \tag{5.7}$$

The ASE denotes the theoretical upper limits on the number of bits that can be transmitted successfully per unit area. Its unit is bps/Hz/m^2.

The above metrics naturally depend on the BS density λ. Our goal is to investigate the exact behavior as a function of different environments and system parameters.

5.3 Densification in the Conventional Scenario

We will first discuss the effect of network densification under the conventional assumptions of cellular networks [9] which are as follows:

1. Standard path-loss model is assumed with path-loss exponent $\alpha > 2$

$$\ell(r) = Cr^{-\alpha}.$$

All links are assumed to undergo Rayleigh fading, i.e., $G \sim \exp(1)$.
2. All BSs are assumed to be homogeneous, i.e. they belong to the same class in terms of key parameters, such as the transmit power.
3. UEs are assumed to have significantly larger density than BSs and their density scales with the BS density as the network densifies. We also assume that BSs have full buffer and are always ready to transmit. Therefore, all BSs are active all the time, i.e., $\lambda_\mathrm{a} = \lambda$.
4. BSs and UEs are at the same height.

5. All BSs are assumed to be deployed according to a stationary Poisson point process (PPP) in 2D space [10].

Under the above assumptions, the SINR coverage probability of a typical UE is given as [10]

$$\begin{aligned} \mathrm{p_c}(\lambda,\alpha) &= \pi\lambda\int_0^\infty \exp\Big(-\pi\lambda v(1+\rho(\gamma_\mathrm{s},\alpha)) - \gamma_\mathrm{s}\sigma^2 v^{\alpha/2}/p\Big)dv \\ &= \pi\int_0^\infty \exp\Big(-\pi v(1+\rho(\gamma_\mathrm{s},\alpha)) - \gamma_\mathrm{s}\sigma^2 v^{\alpha/2}\lambda^{-\alpha/2}/p\Big)dv, \end{aligned} \tag{5.8}$$

where

$$\rho(\gamma,\alpha) = \gamma^{2/\alpha}\int_{\gamma^{-2/\alpha}}^\infty \frac{1}{1+u^{\alpha/2}}\mathrm{d}u. \tag{5.9}$$

For $\alpha = 4$, $\rho(\gamma,\alpha) = \sqrt{\gamma}\arctan\sqrt{\gamma}$. For $\alpha = 2$, $\rho(\gamma,\alpha) = \infty$. In general, $\rho(\gamma,\alpha)$ is monotonic decreasing function of α. The SIR coverage probability can be obtained from (5.8) as

$$\mathrm{p_{cI}}(\lambda,\alpha) = \frac{1}{1+\rho(\gamma_\mathrm{s},\alpha)}. \tag{5.10}$$

5.3.1 Impact of Densification

It is evident from (5.10) that the SIR distribution is invariant of the BS density λ. Figure 5.1 shows the impact of densification on SIR coverage probability, where the same behavior can be observed. This invariance can be understood with the help of the following example.

Example 1 Consider a cellular network in 2D space with BS density λ. At the typical UE (placed at the origin), the SIR is equal to γ with the serving signal power S and the sum interference I. Suppose the network is densified m times resulting in a BS density of $\lambda' = m\lambda$. As a result, all the BSs will statistically move closer to the origin by a factor of $\sqrt{m}$. Therefore, the new serving power will be equivalent in distribution to

$$S' = p_0\|\mathbf{x}_0'\|^{-\alpha} = p_0 m^{\alpha/2}\|\mathbf{x}_0\|^{-\alpha} = m^{\alpha/2}S.$$

Similarly, the sum interference would be equivalent in distribution to

$$I' = \sum_i p_i\|\mathbf{x}_i'\|^{-\alpha} = \sum_i p_i m^{\alpha/2}\|\mathbf{x}_i\|^{-\alpha} = m^{\alpha/2}I.$$

The new SIR is

$$\mathrm{SIR}' = \frac{S'}{I'} = \frac{m^{\alpha/2}S}{m^{\alpha/2}I} = \gamma$$

which has the same form and hence the same distribution as before.

The SINR distribution follows the same behavior as the SIR distribution, except at low BS density. At a lower value of λ, the serving BS, as well as the interfering BSs, is very far from the typical UE. In this case, the interference is negligible compared to noise, which is termed the *noise-limited scenario*. As the network densifies ($\lambda \to \infty$), the serving BS statistically comes closer to the UE and therefore $\mathrm{p_c}$ increases monotonically as can be seen from (5.8) and Fig. 5.1. At large λ, the SINR coverage probability approaches

$$\lim_{\lambda \to \infty} \mathrm{p_c}(\lambda, \alpha) = \mathrm{p_{cI}}.$$

As the BS density λ reaches the critical BS density λ_1, the noise can be neglected (interference-limited scenario, i.e., $\sigma^2 \approx 0$) and $\mathrm{p_c} \approx \mathrm{p_{cI}}$. This critical density depends on the noise power and the BS transmit power. With further increase in the BS density, the densification no longer improves the SINR of a typical UE as the increase in interference power is counterbalanced by the increase in signal power. This observation that SINR in an interference-limited cellular network does not depend on the BS density is often referred to as the *SINR invariance in cellular networks*.

The network densification reduces the user load on each BS without affecting the SINR characteristics. So the network can achieve an approximately linear increase

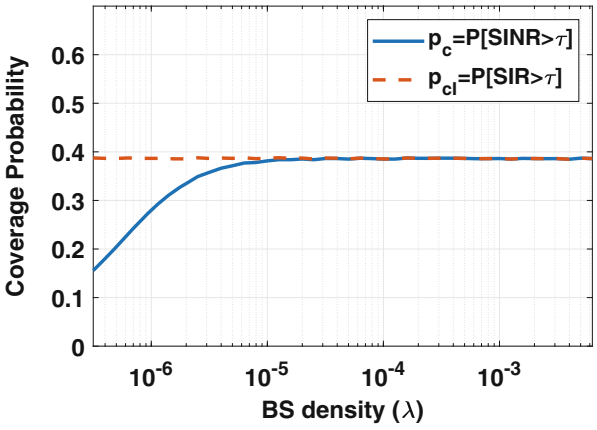

Fig. 5.1 Impact of the BS density on the SINR and SIR coverage probability for a cellular network with the single slope path-loss with $C = 10^{-4}$ and $\alpha = 3$. Here, $\gamma_s = 1$. It can be observed that the SIR distribution is invariant to the BS density

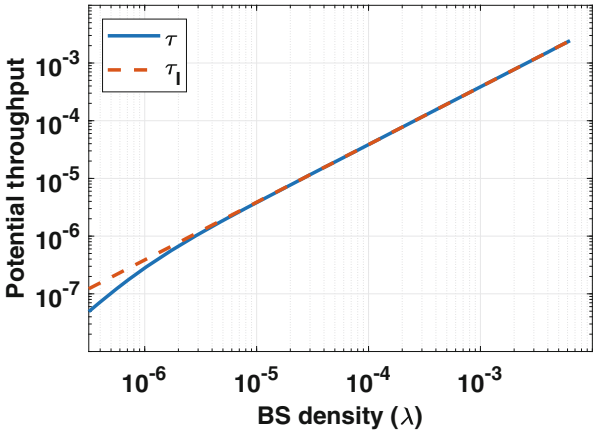

Fig. 5.2 Impact of the BS density on the potential throughput for a cellular network with single slope path-loss with $C = 10^{-4}$ and $\alpha = 3$. Here, $\gamma_s = 1$. The potential throughput grows linearly with the BS densification owing to the SIR invariance observed in Fig. 5.1

in the achievable data rate with the increase in BS density (see Fig. 5.2). As noted before, this gain is termed *cell splitting gain* in the literature. It can be verified using (5.6) and (5.7) that when the SINR invariance property holds, the potential throughput and ASE exhibit linear relation with BS density in the following way:

$$\tau = \lambda \frac{\log(1+\gamma_s)}{1+\rho(\gamma_s,\alpha)} \propto \lambda$$

$$\mathcal{A} = \lambda \mathbb{E}\left[\log(1+\gamma_s)\mathbb{1}\left(\text{SINR} > \gamma_s\right)\right] \propto \lambda.$$

The scaling results in this section are derived based on the assumption that the BSs in the 2D space are distributed according to a homogeneous PPP. However, the real BS deployment is not completely random (nor is it completely regular). Recent studies [11, 12] have shown that a large variety of BS deployment including lattice deployments and hexagonal grid-based deployments have almost similar SIR statistics to that of Poisson deployment, but with a small fixed SIR shift. Moreover, it is known that if all the links in the network undergo significant shadowing that is independent of each other, the network appear Poissonian to the typical UE even if the actual locations are more regular, or even modeled using deterministic grids [13, 14]. Therefore, the results derived in this section are either directly applicable or can be easily modified to apply to more generic scenarios.

Getting back to our main question, the discussion in this section indicates that densifying the network infinitely would keep on increasing the network throughout indefinitely because densification does not impact the coverage probability (equivalently because of the *SINR invariance*). As indicated above already, the SINR invariance property holds for more general setups as well. These include different BS layouts, fading/shadowing assumptions, presence of multiple antennas [15],

distribution of antenna azimuths, and the effect of horizontal sectorization [16], to name a few. In fact, this property is even valid for the multi-tier networks [17]. Specifically, for an interference-limited open access network multi-tier network, adding more tiers or BSs does not affect the SINR distribution at the typical UE. That all being said, it is still important to keep in mind that the SINR invariance property may not universally hold because of which jumping to the conclusion that the network throughput will *always* increase linearly with the addition of BSs may be naïve. At the very least, such statements must be qualified with appropriate assumptions, as we demonstrate next.

5.3.2 Effect of the Dual-Slope Path-Loss Model

In this subsection, we revisit our path-loss assumption to understand its impact on SINR invariance and linear scaling of throughput. The standard path-loss model adopted thus far is widely used by researchers as well as in industry; however, it may not be suitable and valid for modern dense networks [5]. When the distance between BS and UE becomes smaller, the relation of the path-loss with distance may change resulting in the change of path-loss exponent itself. As discussed in detail in [5], the region around a BS can be divided into three regions from the perspective of path-loss modeling:

1. **Ground Fresnel region:** This region is located near the ground surface beyond a significant distance from the transmitter. In this region, the direct and ground reflected rays undergo destructive interference resulting in path-loss exponent close to $\alpha = 4$.
2. **Large-scale interference region:** This region lies beyond a certain distance from the transmitter away from the ground surface. In this region, signals coming from various paths can also add constructively resulting in a lower path-loss exponent ($\alpha \approx 2$).
3. **Small-scale interference region:** This region lies around the transmitter up to some finite distance. Due to the absence of obstacles and additional power received from the reflected paths, the path-loss exponent in this region may decrease below free space path-loss exponent of $\alpha = 2$.

When the link distance between a UE and a BS is small, the UE will be inside the path-loss subduction region of the BS where the path-loss exponent becomes smaller than 2. Having different values of the path-loss exponent in different regions will lead to path-loss exhibiting different slopes in these regions. Such path-loss models are termed *multi-slope path-loss models* in the literature [18]. Given their versatility, e.g., in modeling both indoor and outdoor propagation environments, they have been extensively used in 3GPP standards as well. As an aside for now, note that a probabilistic version of such models has also been proposed and validated for blockage sensitive communications including communications at the millimeter-

wave frequencies. In these models, links follow different slopes according to a probability distribution that depends on the link distance [19].

A specific example of the multi-slope models is the dual-slope model which is simple yet powerful enough to capture the effects of path-loss exponent reduction. Let the path-loss subduction region be represented by the ball of radius R_c around the receiver where R_c is termed the *corner distance*. The dual-slope (power-law) path-loss function is defined as

$$\ell(r) = \begin{cases} C_0 r^{-\alpha_0}, & \text{if } r \leq R_c \\ C_1 r^{-\alpha_1}, & \text{if } r > R_c \end{cases}. \tag{5.11}$$

Therefore, the space around the receiver is divided into two regions. For BSs lying inside the first region R_1 (i.e., $r \leq R_c$), the path-loss exponent is α_0. The path-loss exponent is α_1 for BSs lying in the second region R_2. We consider that $\alpha_0 \leq \alpha_1$. Here, C_1 is chosen such that the path-loss function is continuous at the boundary between these two regions.

To investigate how the dual-slope path-loss model can affect the scaling laws of densification, we will consider the same assumptions as taken in this section (except of course that we will consider a dual-slope path-loss model instead of the standard path-loss model used thus far). Consider again the typical UE at the origin. BSs will be located in either of two different regions R_1 and R_2. Signals from the BSs inside the ball of radius R_c will undergo lower attenuation compared to the BS outside the ball. The average number of BSs in these two regions will be dependent on the BS density, which will eventually impact the coverage probability.

At low BS density $\lambda \to 0$, all BSs will lie in region R_2. Therefore, signals from each of the BSs will undergo attenuation according to path-loss exponent α_1. Hence, the SIR coverage probability of the network would be equal to $\mathrm{p_{cI}}(\gamma_\mathrm{s}, \alpha_1)$ as defined in (5.10). Since the noise would be dominant, the SINR coverage probability will be zero. As BS density increases, initially all BSs would still be located in region R_2. The system will behave exactly like the system with single slope path-loss, and SIR coverage would be invariant of the BS density. However, the SINR coverage would increase with BS density until λ_1 beyond which it would be equal to the SIR coverage probability.

As BS density approaches a critical density λ_3, a few BSs will statistically come closer to the typical UE and would lie in R_1. The serving BS would be one of these BSs as it is the closest BS to the typical UE. At this stage, if the BS density is further increased m times, serving power S will increase by a factor of m^{α_0}, whereas the interfering power I will increase by a factor of m^{α_1} (see Example 1). Here, for the sake of argument we assumed that most of the dominant interferers lie in R_2. Hence, the SIR would decrease by a factor of $m^{\alpha_1 - \alpha_0}$.

As the BS density increases further, another critical density λ_2 approaches where most dominating interfering BSs would lie in the region R_1. At this stage signals from most of the BSs will undergo attenuation according to path-loss exponent α_0. Hence, the SIR coverage probability of the network would be equal to $\mathrm{p_{cI}}(\gamma_\mathrm{s}, \alpha_0)$. If

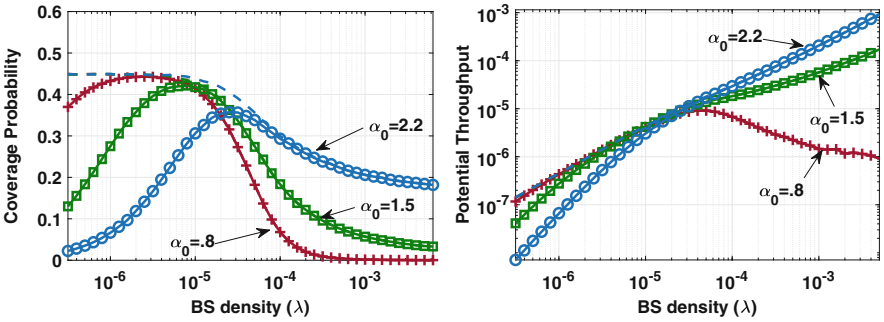

Fig. 5.3 Impact of the BS densification on the SINR and potential throughput under the dual-slope path-loss model with $R_c = 100\,\text{m}$, $C_0 = 10^{-7}$, $\alpha_0 = 0.8, 1.5, 2.2$ and $\alpha_1 = 3.3$. Dashed lines represent respective metrics in the absence of noise

the BS density is further increased m times, serving power S and interfering power I both will increase by a factor of m^{α_0} and SIR would again become invariant of λ. At very high density $\lambda \to \infty$, the SIR and SINR coverage probability of the network would be equal to $\mathrm{p_{cI}}(\gamma_s, \alpha_0)$.

The critical densities λ_3 and λ_2 at which transition from one region to another region occurs depend on the corner distance R_c. The same behavior of the coverage probability with the BS density is also evident in Fig. 5.3.

Clearly, the SINR invariance property no longer holds under the dual-slope path-loss model due to the aforementioned reasons. Another interesting observation one may have is that at very high density, the SINR coverage probability of the network would be equal to $\mathrm{p_{cI}}(\gamma_s, \alpha_0)$, which can be zero depending on the value of α_0. It was shown in [18] that under the dual-slope path-loss model, the SIR and SINR coverage probability of a two-dimensional cellular network goes to zero as $\lambda \to \infty$ when $\alpha_0 \leq 2$. This indicates that the ultra-densification of a network can be harmful to the coverage performance. It was also shown that under the dual-slope model, as $\lambda \to \infty$, the potential throughput τ exhibits the following scaling law:

1. τ grows linearly with λ if $\alpha_0 > 2$,
2. τ grows sublinearly with rate $\lambda^{\left(2-\frac{2}{\alpha_0}\right)}$ if $1 < \alpha_0 < 2$,
3. τ decays to zero if $\alpha_0 < 1$.

Contrary to the conclusions drawn in Sect. 5.3.1, a blind densification of the network may not provide gains proportional to the deployment cost and may in fact be even harmful. Apart from the analytical work, it has also been observed by various empirical studies that densification may cause the network throughput to fall and even crash [20]. With these seemingly conflicting conclusions, it is clear that one needs a more careful look at potential factors that may impact the densification gain, which is the topic of the next section.

5.4 Factors Affecting the Densification Gain

In the last section, we saw that adopting a more realistic path-loss model, such as the dual-slope model, changed the conclusions of the densification gain significantly. The naïve assumption that densification can infinitely increase the potential throughput and ASE is clearly not valid. In fact, densification may cause throughput to fall and even crash if done beyond a limit. Apart from path-loss model, there are many other factors that affect the scaling behavior of the performance with densification. In this section, we discuss some of these factors in detail.

5.4.1 Path-Loss Models

We have already seen how incorporating two slopes in the path-loss model disrupts the scaling of system performance with densification. There exist other realistic path-loss models suitable for various propagation environment which are discussed below.

Multi-slope Path-Loss Model

The dual-slope model can be extended to a general N-slope path-loss to include propagation environments where more than two path-loss subduction regions exist [21]. The N-slope path-loss is defined as

$$\ell(r) = \begin{cases} \ell_0(r) = C_0 r^{-\alpha_0} & \text{if } r \in [0 = R_0, R_1) \\ \cdots \\ \ell_n(r) = C_n r^{-\alpha_n} & \text{if } r \in [R_n, R_{n+1}) \\ \cdots \\ \ell_{N-1}(r) = C_{N-1} r^{-\alpha_{N-1}} & \text{if } r \in [R_{N-1}, R_N = \infty) \end{cases} \tag{5.12}$$

Here, $C_0 = 1$ is the near-field gain and $C_n = \prod_{i=1}^{n} R_i^{\alpha_i - \alpha_{i-1}}$ to ensure that path-loss is continuous at the boundaries of the adjacent regions. Also, $0 = R_0 < R_1 < \cdots < R_N = \infty$ are corner distances and $0 \leq \alpha_0 \leq \alpha_1 \leq \cdots \leq \alpha_{N-1}$ are path-loss exponents for N regions. We assume that $\alpha_{N-1} > 2$ to ensure that the sum interference at finite BS density is bounded. We do not require any additional conditions on any other path-loss exponents as the number of BSs lying in all other regions is almost surely finite and, hence, the interference is also almost surely finite. When $N = 2$, this model reduces to the special case of the dual-slope path-loss model (5.11).

As described earlier, the SIR and SINR invariance properties no longer hold for multi-slope models. Initially, SINR improves with densification before the BS

density hits the critical density λ_1 after which the network becomes interference limited. After this, SINR and SIR coverage probability become the same. As $\lambda \to \infty$, the coverage probability approach $p_{cI}(\alpha_0)$ which depends only on the value of α_0 regardless of the number of slopes. Therefore, asymptotic behavior of coverage and potential throughput is exactly the same as the one described above for the dual-slope model.

Probabilistic Two-Regime Model

Given the increasing relevance of millimeter wave communications in cellular networks, it is important to carefully incorporate the blockage sensitivity of these frequencies in the propagation models. In the context of this discussion, it is important to distinguish the line-of-sight (LOS) and non-LOS (NLOS) links as they differ significantly in their propagation characteristics. To model such propagation, a probabilistic two-regime model has been proposed [19, 22] where a link can be LOS or NLOS randomly according to a probability distribution p_L. This LOS probability p_L depends on the link distance. If the link between a transmitter and a receiver located at a distance of r is LOS, it follows the following path-loss model:

$$\ell_L(r) = C_L r^{-\alpha_L},$$

whereas a NLOS link suffers with the following path-loss

$$\ell_N(r) = C_N r^{-\alpha_N}.$$

The complete model is given as

$$\ell(r) = \begin{cases} \ell_L(r) = C_L r^{-\alpha_L} & \text{with probability } p_L(r) \\ \ell_N(r) = C_N r^{-\alpha_N} & \text{with probability } 1 - p_L(r) \end{cases}.$$

There are two distinguishing properties of these model compared to the two-slope model:

1. The two regimes in this model are probabilistic and can overlap in space, while two regions in the two-slope model are deterministic and mutually exclusive.
2. There is no continuity condition on gains C_L and C_N. LOS and NLOS links can have different gains event at the unit distance [23].

Throughout this discussion, we assume that each UE is associated with the BS providing the smallest path-loss.

The behavior of SIR and SINR coverage probability with densification under the two-regime model is similar to the two-slope model with some differences. At the low BS density, all BSs will be NLOS. Therefore, signals from each of the BSs will undergo attenuation according to path-loss exponent α_N. Hence, the

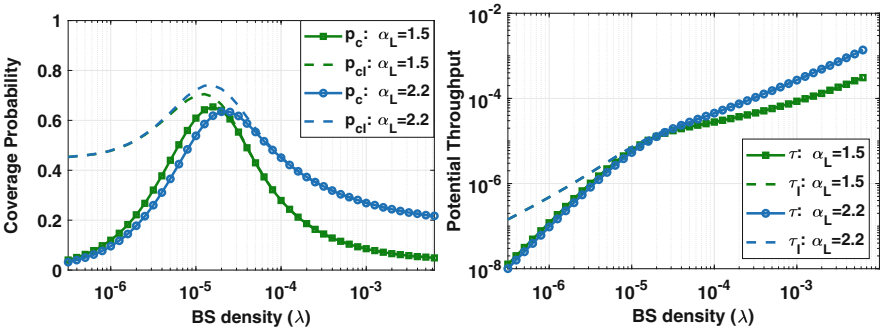

Fig. 5.4 Impact of the BS densification on the potential throughput under the probabilistic two-regime model with $\alpha_{\mathrm{L}} = 1.5, 2.2$, $\alpha_{\mathrm{N}} = 3.3$, $C_{\mathrm{L}} = 10^{-6}$ and $C_{\mathrm{N}} = 10^{-7}$. Here, the LOS probability model is assumed to be exponential i.e. $p_{\mathrm{L}}(r) = \exp(-\beta r)$ with $\beta = 1/144\,\mathrm{m}^{-1}$. Dashed lines represent respective metrics in the absence of noise

SIR coverage probability of the network would be constant at $\mathrm{p_{cI}}(\gamma_{\mathrm{s}}, \alpha_{\mathrm{N}})$. Since the noise would be dominant, SINR coverage probability will increase with BS density. As the BS density increases, a few BSs will become LOS to the typical UE. The serving BS would most likely be one of these BSs. Since the gain of the LOS link is more than the NLOS link, SIR coverage probability would improve. At this stage, if the BS density is further increased, the probability of the serving BS to be LOS increases, and hence the SIR coverage probability improves. After a critical density of BSs, further increase in the BS density causes interfering BSs to become LOS also. This increases the interference severely causing SIR to go down. As the BS density increase further, most dominating interfering BSs would become LOS. At this stage, signals from most of the BSs will undergo attenuation according to path-loss exponent α_{L}. Hence, the SIR coverage probability of the network would approach $\mathrm{p_{cI}}(\gamma_{\mathrm{s}}, \alpha_{\mathrm{L}})$ and becomes constant at this level. The above discussion indicates the existence of an optimal density λ_{opt} of that BSs that would maximize the coverage probability (see Fig. 5.4). Densification beyond this optimal density would hurt SIR and even makes it fall to zero if $\alpha_{\mathrm{L}} < 2$.

The SIR degradation also impacts the throughput scaling. For some values of $\alpha_{\mathrm{L}} < 2$ and γ_{s}, the densification beyond λ_{opt} may reduce the potential throughput (see Fig. 5.4). Asymptotic scaling of potential throughput with densification is the same as scaling under multi-slope model with $\alpha_0 = \alpha_{\mathrm{L}}$.

General Multi-regime Multi-slope Probabilistic Path-Loss Model

The multi-slope path-loss model and the probabilistic path-loss model can be combined into a general multi-regime multi-slope path-loss model which is defined as [24, 25]

$$\ell(r) = \begin{cases} \ell_1(r) = \begin{cases} \ell_{1\mathrm{L}}(r), & \text{with probability } p_{1\mathrm{L}}(r) \\ \ell_{1\mathrm{N}}(r), & \text{with probability } (1 - p_{1\mathrm{L}}(r)) \end{cases} & \text{if } 0 \le r \le R_1 \\ \ell_2(r) = \begin{cases} \ell_{2\mathrm{L}}(r), & \text{with probability } p_{2\mathrm{L}}(r) \\ \ell_{2\mathrm{N}}(r), & \text{with probability } (1 - p_{2\mathrm{L}}(r)) \end{cases} & \text{if } R_1 \le r \le R_2 \\ \vdots & \vdots \\ \ell_m(r) = \begin{cases} \ell_{m\mathrm{L}}(r), & \text{with probability } p_{m\mathrm{L}}(r) \\ \ell_{m\mathrm{N}}(r), & \text{with probability } (1 - p_{m\mathrm{L}}(r)) \end{cases} & \text{if } r > R_{m-1} \end{cases} \tag{5.13}$$

where $\ell_{i\mathrm{L}}(r)$ and $\ell_{i\mathrm{N}}(r)$ are the path-loss functions for the LOS and NLOS links, respectively, in ith region. $P_{i\mathrm{L}}(r)$ is the ith piece LOS probability function. $\ell_{i\mathrm{L}}(r)$ and $\ell_{i\mathrm{N}}(r)$ are given as

$$\ell_{i\mathrm{L}}(r) = C_{i\mathrm{L}} r^{-\alpha_{i\mathrm{L}}}, \tag{5.14}$$

$$\ell_{i\mathrm{N}}(r) = C_{i\mathrm{N}} r^{-\alpha_{i\mathrm{N}}}. \tag{5.15}$$

where the parameters can be chosen to match the empirical data. This model is consistent with the ones adopted in 3GPP simulations. We discuss two special cases of this model which are mentioned in 3GPP documents and have been used in 3GPP simulations to evaluate the performance of cellular networks.

3GPP-Model-1

First, we consider a 3GPP model given as [26]

$$\ell_n(r) = \begin{cases} C_{\mathrm{L}} r^{-\alpha_{\mathrm{L}}} & \text{with probability } p_{\mathrm{L}}(r) \\ C_{\mathrm{N}} r^{-\alpha_{\mathrm{N}}} & \text{with probability } (1 - p_{\mathrm{L}}(r)) \end{cases}. \tag{5.16}$$

with linear LOS probability function [27],

$$p_{\mathrm{L}}(r) = \begin{cases} 1 - r/D & \text{when } 0 \le r \le D \\ 0 & \text{when } r > d_1 \end{cases}.$$

Note that the model given in (5.16) is the special case of (5.13) where $m = 2$, $\ell_{1\mathrm{L}}(r) = \ell_{2\mathrm{L}}(r) = C_{\mathrm{L}} r^{-\alpha_{\mathrm{L}}}$, $\ell_{1\mathrm{N}}(r) = \ell_{2\mathrm{N}}(r) = C_{\mathrm{N}} r^{-\alpha_{\mathrm{N}}}$, $p_{1\mathrm{L}}(r) = 1 - \frac{r}{D}$ and $p_{2\mathrm{L}}(r) = 0$. This model was proposed for dense small cell networks.

3GPP-Model-2

The second model considered here is proposed in [26]. This model has the same path-loss function as (5.16) but with an exponential LOS probability function:

$$p_{\mathrm{L}}(r) = \begin{cases} 1 - 5\exp\left(-D_1/r\right) & \text{when } 0 \le r \le D \\ 5\exp\left(-r/D_2\right) & \text{when } r > D \end{cases},$$

where $D = D_1/\ln(10)$. This model is the special case of (5.13) where $m = 2$, $\ell_{1\mathrm{L}}(r) = \ell_{2\mathrm{L}}(r) = C_{\mathrm{L}} r^{-\alpha_{\mathrm{L}}}$, $\ell_{1\mathrm{N}}(r) = \ell_{2\mathrm{N}}(r) = C_{\mathrm{N}} r^{-\alpha_{\mathrm{N}}}$, $p_{1\mathrm{L}}(r) = 1 - 5\exp(-D_1/r)$, and $p_{2\mathrm{L}}(r) = 5\exp(-r/D_2)$.

Figure 5.5 shows the behavior of potential throughput with densification under the two 3GPP path-loss models. The key observations can be summarized as follows. When the network is sparse, the potential throughput quickly increases with BS density. This is due to the fact that the network is noise-limited, and thus adding more BSs immensely benefits the throughput. When the network reaches the practical density (as expected in 4G/5G systems), the scaling trend of the potential throughput is very interesting. Initially throughput exhibits a slowing-down in the rate of growth or even a decrease due to the fast decrease of the coverage probability. As BS density further increases, the growth rate of the throughput picks up. This is because the coverage probability remains almost constant in this region (but at a much lower value than before). The behavior of the throughput depends on the characteristics of the LOS and the NLOS path-loss. The larger the difference between the LOS and the NLOS path-loss exponents, the more the throughput suffers in transition region due to more drastic transition of interference from the NLOS transmission to the LOS transmission. This asymptotic behavior is similar to what is seen in the previous models.

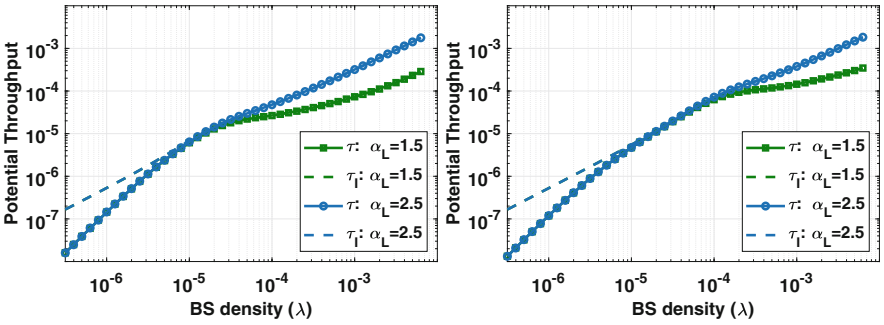

Fig. 5.5 The impact of the BS densification on the potential throughput under the 3GPP-Model-1 and 3GPP-Model-2 with $\alpha_{\mathrm{L}} = 1.5,\ 2.5$, $\alpha_{\mathrm{N}} = 3.75$, $C_{\mathrm{L}} = 10^{-10.38+3\alpha_{\mathrm{L}}}$ and $C_{\mathrm{N}} = 10^{-14.54+3\alpha_{\mathrm{N}}}$. Additionally, for 3GPP-Model-1, $D = 300\,\mathrm{m}$ and for 3GPP-Model-2, $D_1 = 156\,\mathrm{m}$ and $D_2 = 30\,\mathrm{m}$. Here, $\gamma_{\mathrm{s}} = 1$. Dashed lines represent respective metrics in the absence of noise

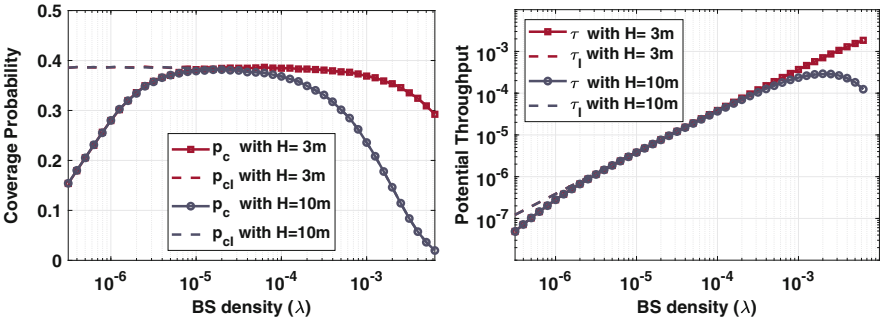

Fig. 5.6 Impact of the BS density on the coverage probability and potential throughput for a cellular network with height difference of H under the single slope path-loss with $C = 10^{-4}$ and $\alpha = 3$. Here, $\gamma_s = 1$. It can be observed that the SIR distribution is invariant to the BS density. Dashed lines represent respective metrics in the absence of noise

5.4.2 *Height Difference Between BS and UE Antennas*

In deriving the scaling behavior of densification until now, we have assumed that the height of the BSs and UEs are the same. In a practical scenario, there may be some height difference H between the heights of the BSs and UEs. Figure 5.6 shows how SINR and throughput scales with density when H is 3m and 10m. The path-loss model assumed for these plots is the standard single slope path-loss model. We observe that at large density, both the SIR coverage probability and the potential throughput decrease and eventually crash to zero even for path-loss exponent $\alpha > 2$. This is in contrast with results obtained for the scenario with zero height difference (see Figs. 5.1 and 5.2), where throughput was observed to grow linearly with the BS density for the same value of the path-loss exponent. This can be understood by the following example.

Example 2 Consider a 2D cellular network where BSs have height H and UEs are at the ground level. Consider the ith BS at a 2D distance (i.e., distance along the ground) r_i from the typical UE. Hence, the 3D distance between the two is $\sqrt{r_i^2 + H^2}$. The average receiver power at the UE from this BS is $pC(r_i^2 + H^2)^{-\alpha}$. Hence, the SIR is given as

$$\text{SIR} = \frac{(r_0^2 + H^2)^{-\alpha/2}}{\sum_i (r_i^2 + H^2)^{-\alpha/2}}.$$

Note that a densification by a factor of m is statistically equivalent to reduction in all 2D distances by a factor $\sqrt{m}$. The new SIR at the typical UE would be equivalent in distribution to

$$\text{SIR}' = \frac{((r_0/\sqrt{m})^2 + H^2)^{-\alpha}}{\sum_i ((r_i/\sqrt{m})^2 + H^2)^{-\alpha}}$$
$$= \frac{((r_0)^2 + mH^2)^{-\alpha}}{\sum_i ((r_i)2 + mH^2)^{-\alpha}}.$$

If $H = 0$, the above would be equal to the original SIR itself. However, when H is non-zero, for large m,

$$\text{SIR}' \approx \frac{(mH^2)^{-\alpha}}{\sum_i (mH^2)^{-\alpha}} = \frac{1}{\sum_i 1} \to 0$$

as there are many BSs around the UE at distance H for large m.

As we increase the BS density, BSs statistically comes closer to the typical UE. If there is a height difference between a BS and the UE, the 3D distance between them cannot go to zero even if the BS density goes to infinity. In fact, the distance between the BS and UE will be lower bounded by the difference in their heights. Therefore the signal power from each BS cannot be larger than $pH^{-\alpha}$. Consequently, at a large density, signal power from each of the serving BSs and each interfering BS would approach this value and result in zero coverage probability. As a result, potential throughput and ASE would also fall to zero. One way to avoid ASE crash is by avoiding the cap on the signal power of the serving BSs, which can be done by deploying BSs at the same height as UE. If that is not possible, reducing the antenna height of BS to that of UE antenna height can delay this crash, but cannot completely avoid it.

5.4.3 Scaling of the UE Density

While showing the SINR invariance for single slope path-loss model, we have assumed that the UE density is significantly larger than the BSs or scales with network densification so that all BSs are active all the time. In practice, the UE density is finite. As the BS density reaches the UE density level, some BSs will not have any UEs to serve and can hence be put into idle mode to avoid interfering with the UEs of the other cells and reduce their energy consumption. This will naturally affect the interference distribution and hence the system throughput.

We will continue to use the PPP assumption for the BS deployment here to provide insights into the performance trends under finite UE density. In particular, assume that the BSs are deployed according to a homogeneous PPP with density λ. The typical UE is associated with the closest BS. The rest of the BSs are interfering. It was shown in [28] that the probability that a typical BS is turned-on (which is equal to the probability that a typical BS has at least one UE in its cell) is given as

$$p_{\text{on}} = 1 - 3.5^{3.5}\left(3.5 + \frac{\lambda_u}{\lambda}\right)^{-3.5}.$$

Hence, the active BS density is given as $\lambda_a = \lambda p_{\text{on}}$. It can be quickly verified that

$$p_{\text{on}} \rightarrow 0 \text{ and } \lambda_a \rightarrow \lambda_u \text{ as } \lambda \rightarrow \infty. \tag{5.17}$$

Equation (5.8) can be modified to get the SINR coverage probability for the finite UE density scenario as

$$\begin{aligned} \mathrm{p_c}(\lambda, \alpha) &= \pi\lambda \int_0^\infty \exp\left(-\pi\lambda v(1 + p_{\text{on}}\rho(\gamma_s, \alpha)) - \gamma_s \sigma^2 v^{\alpha/2}/p\right) dv \\ &= \pi \int_0^\infty \exp\left(-\pi v(1 + p_{\text{on}}\rho(\gamma_s, \alpha)) - \gamma_s \sigma^2 v^{\alpha/2}\lambda^{-\alpha/2}/p\right) dv, \end{aligned} \tag{5.18}$$

and the SIR coverage probability is given as

$$\mathrm{p_{cI}} = \frac{1}{1 + p_{\text{on}}\rho(\gamma_s, \alpha)}. \tag{5.19}$$

The expression (5.18) indicates that the distribution of distance from the serving BS is the same as in the case with infinite UE density. This is because the typical UE still connects to the closest BS from the original PPP. However, compared to the infinite UE density case, the interfering BS density reduces to λ_a when the UE density is finite and therefore the aggregate interference is less.

Note from (5.17) and (5.19) that as $\lambda \rightarrow \infty$, $\mathrm{p_{cI}} \rightarrow 1$. This is due to the fact that as the network densifies, the serving BS comes statistically closer to the UE while interfering BS density remains constant at λ_u. This indicates that the SINR invariance does not hold here and densification can in fact improve coverage gains. However, as we will see next, the throughput tells a very different story. For finite UE density case, the potential throughput is given as

$$\tau = \lambda_a \log(1 + \gamma_s)\mathrm{p_c}(\gamma_s, \alpha).$$

Note the scaling term λ_a instead of λ owing to the fact that the number of transmissions is equal to the number of active BSs. As the network is densified, the coverage probability increases, but the τ is still upper bounded by $\lambda_u \log(1 + \gamma_s)$. Once the throughput approaches this value, further densification will not give any gains [29]. The same behavior can be observed in the simulation results shown in Fig. 5.7.

Apart from the theoretical bounds on achievable rate, the assumption of finite UE density also raises some practical issues, e.g., loss of multi-user diversity [7]. At large BS density, there would be only one UE in the cell of each active BS.

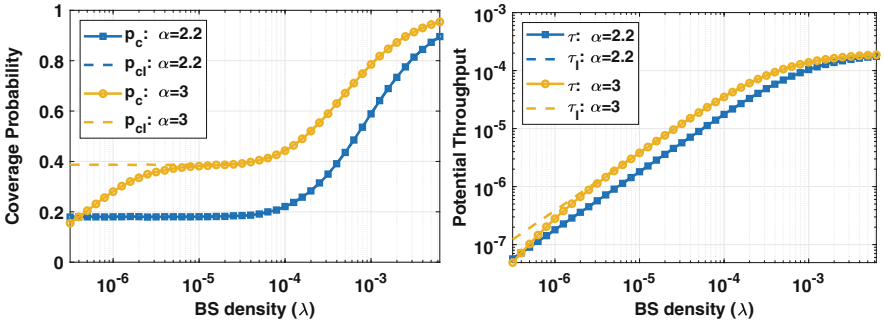

Fig. 5.7 Scaling of the coverage probability and potential throughput with the BS density for a cellular network with the fixed UE density of 200 UE/km^2, under the single slope path-loss. Here, $\gamma_s = 1$, $C = 10^{-4}$ and the path-loss exponent values are taken as $\alpha = 2.2$ and 3. Dashed lines represent respective metrics in the absence of noise

Therefore, BSs lose the opportunity to select the best UE among all connected UEs, which can reduce the practical gains achievable via densification [30].

5.4.4 Traffic Characteristics

The UE density represents the average active traffic load in the network. We have seen in the previous subsection that this average active traffic load has a significant impact on the densification gain. Apart from the average characteristics, instantaneous traffic patterns will naturally have an impact on the densification conclusions as well.

The activity time of a BS depends on the traffic pattern of the UEs served by it. In case of bursty traffic, or when the traffic is sparsely distributed over space, many BSs will not have any traffic requests in their queue. This can reduce the sum interference significantly even when the BS density is high. When there are few active UEs in any BS cell, the downlink and uplink traffic demands become highly dynamic in that cell [7]. As another consequence, the ratio of downlink and uplink traffic becomes highly asymmetric over the space. In such scenario, the same division of resources between uplink and downlink for each cell may lead to inefficient utilization of available resources. To tackle such traffic, dynamic time-division duplex (TDD) has emerged as a promising technology for ultra-dense networks. Dynamic TDD can be seen as a hybrid technology between the conventional half-duplex and the emerging full duplex networks. In dynamic TDD, each BS has the flexibility to choose a custom division of resources between downlink and uplink to match the traffic demands in its cell. However, since the resource division is no longer synchronized among neighboring cells, the communication suffers from cross-link interference. For example, the uplink transmission in a cell may face strong interference from

the downlink transmission occurring in the neighboring cell which may degrade the reception significantly.

Since uplink and downlink interference distributions are very different from each other, they can affect the densification gains. As network densifies, downlink interference can severely degrade uplink performance and may render uplink communication unusable. It has also been shown that Dynamic TDD can give significant gains when the mean number of uplink (or downlink) UEs per active BS is less than 1 [31]. This scenario can occur when the uplink/downlink traffic is asymmetric and the network density reaches the UE density. This performance can be improved with the help of interference cancellation and UE power boosting. However, at high network density, the implementation of these schemes may require large overhead, which can eat away all the gains.

5.4.5 Blockages

Blockages can affect both the serving and interfering links, especially at very high transmission frequencies, such as millimeter waves. The impact of blockages can be modeled using the probabilistic two regime (LOS/NLOS) model discussed already in Sect. 5.4.1. Therefore, there exists an optimal BS density at which coverage probability is maximized. This optimal density λ_a ensures that there is a significant probability of having one LOS serving BS while restricting the probability of having a LOS interfering BS. Therefore, λ_a depends on the blockage probability. As blockage probability increases, adequate densification is required to increase the probability of getting at least one BS as LOS which can act as the serving BS [32]. The readers are advised to refer to Sect. 5.4.1 for a more detailed discussion.

5.4.6 Deployment

Most of the existing literature focusing on densification gains considers BS deployment in 2D space. However, in cities (especially, dense downtown areas), BSs are also deployed in the vertical direction, for example, one at each floor of the building. These BSs mainly include user-installed small cells. A user located in the middle floor of a tall building in such an urban environment would see an appreciable number of BSs in every direction. This would seem like a 3D deployment of BSs to these users. Moreover, the increasing maturity of unmanned aerial vehicle (UAV)-assisted communication networks also increases the relevance of 3D networks [33]. Naturally, 3D deployments will have an impact on the densification gains of cellular networks.

The work [34] discussed scaling of densification for general BS deployment in d dimension. For a general d-D network, the required condition for the bounded

interference (in almost sure sense) is $\alpha > d$. If the path-loss exponent $\alpha \leq d$, the coverage probability and throughput are both 0. Under the dual-slope path-loss model, the SIR and SINR coverage probability of a general $d-$D system go to zero as $\lambda \to \infty$ for $\alpha_0 \leq d$. As $\lambda \to \infty$, the potential throughput τ exhibit the following scaling behavior:

1. τ grows linearly with λ if $\alpha_0 > d$,
2. τ grows sublinearly with rate $\lambda^{\left(2-\frac{d}{\alpha_0}\right)}$ if $\frac{d}{2} < \alpha_0 < d$,
3. τ decays to zero if $\alpha_0 < \frac{d}{2}$.

For the 3D scenario, the critical value of α_0 is 3. In other words, $\mathrm{p_c}$ goes to zero for $\alpha_0 \leq 3$ as BS density goes to infinity. Potential throughput goes to zero if $\alpha_0 < 1.5$. When $1.5 < \alpha_0 < 3$, densification gives sublinear gains to the potential throughput. It is very common for the path-loss exponent of short range systems to be less than these α_0 values, so this is seemingly an important concern for future ultra-dense networks. Figure 5.8 shows the behavior of the coverage probability and potential throughput for a 3D BS deployment with the network density.

5.4.7 *Directional Communication*

The use of multiple antennas can help improve the performance of wireless systems by providing directionality gains. Directional communication increases the serving power and reduces the aggregate interference. For higher frequencies such as the millimeter waves, directional communication is essential to facilitate reliable communication owing to high propagation losses. As the directionality can improve

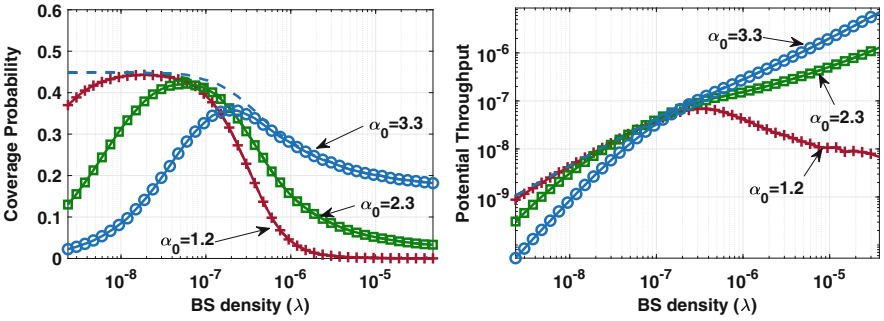

Fig. 5.8 Impact of the BS densification on the SINR and potential throughput for a 3D BS deployment. The path-loss is dual-slope with $R_c = 100\,\mathrm{m}$, $C_0 = 10^{-7}$, $\alpha_0 = 1.2, 2.3, 3.3$, and $\alpha_1 = 4.95$. Dashed lines represent respective metrics in the absence of noise. The behavior is similar to that observed for 2D deployments; however, the critical values of parameters have changed. Dashed lines represent respective metrics in the absence of noise

SINR coverage, network densification gains would increase especially at high densities [35]. Although the introduced directional gain doesn't change the inherent behavior of the scaling laws under densification, it can delay the potential SINR and throughput crashes.

5.4.8 Association Criterion

For systems under single-slope path-loss, we have considered the association criterion that a UE is associated with the BS which provides the highest average received power. There are other association criteria that can be used based on the design objective. One such example is the instantaneous signal power-based association which includes the random fading into consideration while selecting the serving BS. Figure 5.9 shows the comparison of these two association criteria. Instantaneous criterion provides a certain gain to SIR coverage probability. However, at lower density, this gain is not visible in SINR coverage probability. As network densifies, the association criterion needs to be carefully selected.

For millimeter wave systems, an appropriate path-loss model to consider is the probabilistic LOS/NLOS regime model discussed in Sect. 5.4.1. As has been done for the other path-loss models until now, one possible association criterion is to select the closest BS. Figure 5.10 presents scaling results under closest distance-based association compared to the highest average received power-based association. We can observe here that at moderate density of BSs, the distance-based association degrades SINR coverage probability significantly. We also observe that there may not be any optimal BS density which maximizes SIR unlike the case where received power-based association is applied.

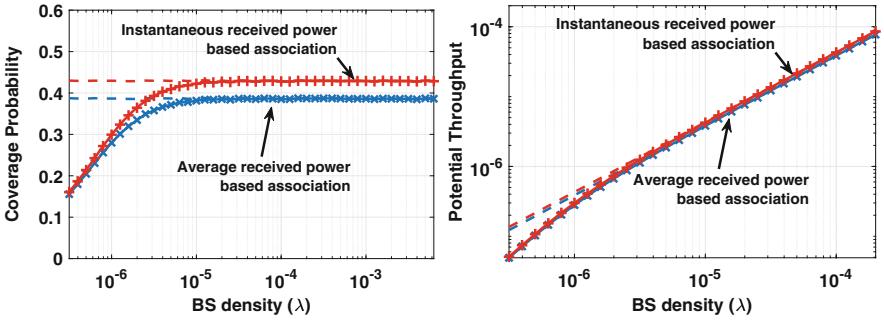

Fig. 5.9 Impact of different association criteria on the densification gain for a cellular network under single slope path-loss model with $C = 10^{-4}$ and $\alpha = 3$. Here, $\gamma_s = 1$. Dashed lines represent respective metrics in the absence of noise

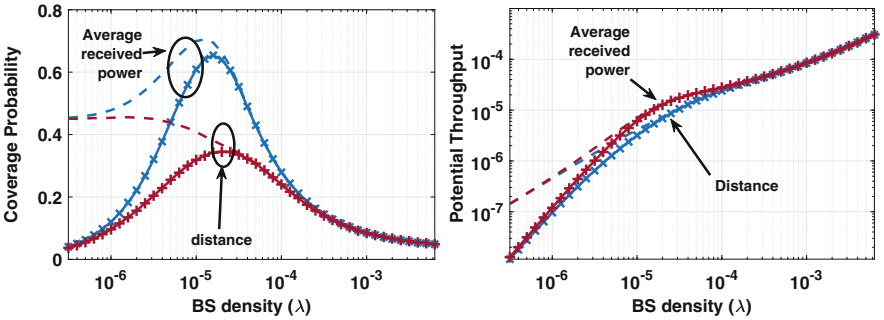

Fig. 5.10 Impact of the implementation of different association criteria on the densification gain for a cellular network under the probabilistic two-regime path-loss model with $\alpha_{\mathrm{L}} = 1.5$, $\alpha_{\mathrm{N}} = 3.3$, $C_{\mathrm{L}} = 10^{-6}$, and $C_{\mathrm{N}} = 10^{-7}$. Here, the LOS probability model is assumed to be exponential, i.e., $p_{\mathrm{L}}(r) = \exp(-\beta r)$ with $\beta = 1/144\,\mathrm{m}^{-1}$. $\gamma_{\mathrm{s}} = 1$. Dashed lines represent respective metrics in the absence of noise

5.4.9 Access Restrictions in Multi-tier Networks

As discussed in Sect. 5.1, early deployments of cellular networks involved carefully planned set of large tower-mounted macrocells. As the data demand increased, both service providers and end users have started deploying small BSs, typically in the form of micro-, pico-, and femto-cells, which may share the same spectrum. Each of the tiers is distinguished by its transmit power, BS density, transmission techniques, height, and deployment. Such network consisting of multiple classes (tiers) of BSs is known as a *heterogeneous network (HetNet)* [17, 36]. In the presence of other BS tiers, a cellular network will suffer from additional interference created by their transmissions. Oftentimes, however, UEs of a cellular network may be allowed to connect and use the services of small cells, which can provide additional gain. Whether or not a UE is allowed to connect to small cells (some of which may be owned by the other users) is determined by the *access strategy* [28].

In open access, a UE with subscription to the considered network is allowed to connect to any of the tiers without any restriction. On the other hand, in a closed access strategy, the UE is allowed to connect only to a selected tiers. This access method is mainly used in private infrastructures, e.g., to provide services to its members in a private club. Closed access strategies are often inspired by finite backhaul capacity, security concerns, and the need to reduce the number of hand-offs experienced by UEs as well as the associated signaling overhead.

In both the access schemes, the subscribed tier and all the other tiers will cause interference to the typical UE as they all use the same spectrum. However, in open access, the associated BS is the *best* BS among BSs of all tiers for this UE. On the other hand, in closed access, the associated BS is the *best* BS among all the BSs of the tiers that the UE is subscribed to. It is indeed possible in this case that there is

a BS in another tier than can provide better service to the UE, but the UE may be restricted to access it. Therefore, closed access by design leads to a lower coverage probability in this setting. To understand the behavior, we go back to the simple model. Let us assume a K tier network with BSs of each tier deployed according to an independent PPP. For simplicity, we will take identical tiers, however each having different BS density λ_i. Consider a UE of the first network. Denote the set of tiers that allow connection to this UE by $\mathcal{I}$. Suppose the combined density of the tiers that it can connect to is $\mu_1 = \sum_{\mathcal{I}} \lambda_i$ while the combined density of tiers closed to this UE is $\mu_2 = \sum_{[1:K]\setminus\mathcal{I}} \lambda_i$. Let use consider single slope path-loss propagation with α path-loss exponent. Under the above assumptions, the SINR coverage probability of a typical UE is given as [37]

$$\mathrm{p_c}(\lambda, \alpha) = \pi \mu_1 \int_0^\infty \exp\Big(-\pi v(\mu_1 + \mu_1 \rho(\gamma_\mathrm{s}, \alpha) + \mu_2 \beta(\alpha)) - \gamma_\mathrm{s} \sigma^2 v^{\alpha/2}/p\Big) dv \tag{5.20}$$

where

$$\rho(\gamma, \alpha) = \gamma^{2/\alpha} \int_{\gamma^{-2/\alpha}}^\infty \frac{1}{1+u^{\alpha/2}} \mathrm{d}u, \quad \beta(\alpha) = \gamma_\mathrm{s}^{2/\alpha} \int_0^\infty \frac{1}{1+u^{\alpha/2}}. \tag{5.21}$$

For $\alpha = 4$, $\rho(\gamma, \alpha) = \sqrt{\gamma} \arctan \sqrt{\gamma}$ and $\beta(\alpha) = \sqrt{\gamma}\pi/2$. For $\alpha = 2$, $\rho(\gamma, \alpha) = \beta(\alpha) = \infty$. The SIR coverage probability of the typical UE is

$$\mathrm{p_{cI}}(\lambda, \alpha) = \frac{1}{1 + \rho(\gamma_\mathrm{s}, \alpha) + \mu_2/\mu_1 \beta(\alpha)} \tag{5.22}$$

In symmetrical networks where each tier densifies equally ($\lambda_i = \lambda \; \forall i$), the closed and open access coverage probability are given as

$$\mathrm{p_{cI,closed}}(\lambda, \alpha) = \frac{1}{1 + \rho(\gamma_\mathrm{s}, \alpha) + (K-1)\beta(\alpha)} \leq \frac{1}{1 + K\rho(\gamma_\mathrm{s}, \alpha)}$$

$$\mathrm{p_{cI,open}}(\lambda, \alpha) = \frac{1}{1 + \rho(\gamma_\mathrm{s}, \alpha)}$$

Closed access can reduce the coverage by factor $\approx K$ as seen in Fig. 5.11. However, in both cases, SIR coverage probability is independent of λ.

In asymmetric networks where one tier has higher density than the other, closed access can severely affect the performance of the latter network. Observe the factor μ_2/μ_1 in (5.22). If μ_1 is fixed, densification of the second network can drastically decrease coverage probability of the first tier under closed access scheme. However, under open access, coverage probability does not depend on this densification. To show this, we consider a two-tier network where the density of the first network is fixed at 30 BS km^2. We densify the second network and the behavior of $\mathrm{p_c}$ and τ is

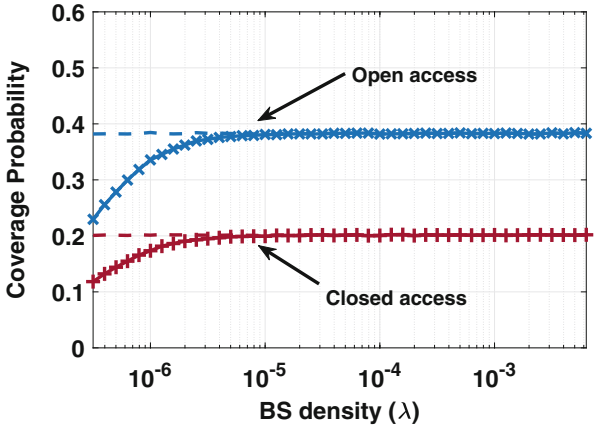

Fig. 5.11 Scaling of the coverage probability with network densification for a two-tier cellular network with different access restrictions. Both networks have the same BS density while densification. The path-loss model is taken as the single slope path-loss with $C = 10^{-4}$ and $\alpha = 3$. Here, $\gamma_s = 1$

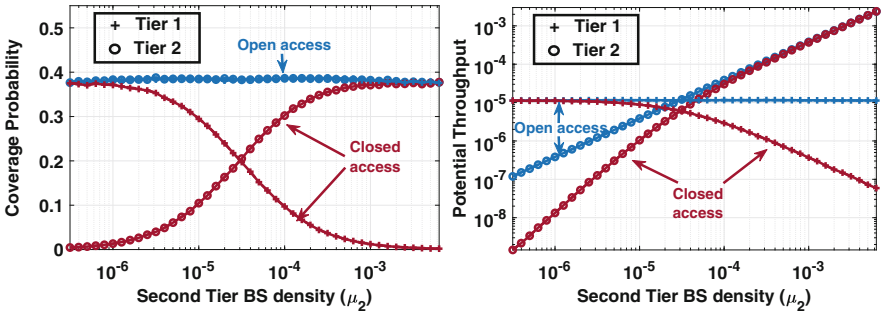

Fig. 5.12 Impact of the BS densification of the second tier on the coverage probability and potential throughput of the first tier in a two-tier asymmetric cellular network with different access restrictions. First tier is fixed density at 30BS/km^2, while the second tier's BS density is varied. The path-loss model is taken as the single slope path-loss with $C = 10^{-4}$ and $\alpha = 3$. Here, $\gamma_s = 1$. Dashed lines represent respective metrics in the absence of noise

shown in Fig. 5.12. In open access, the SIR is invariant to the network density for both the tiers. In closed access, densification of the second tier will cause the first tier's coverage to fall to zero. This is due to the fact that densification of the second tier will increase the interference, while the serving power depends on the first tier's BS density which is fixed. However, the coverage probability of the second tier increases with its densification.

The potential throughput of the first tier remains constant in open access, while it falls to zero in the closed access. However, the throughput of the second tier linearly increases with densification in both access schemes.

This discussion indicates that some tiers are closed for access to some UEs; the densification of one tier can severely affect the other tiers. Therefore, it is important to coordinate the densification of different tiers to ensure reasonable network performance.

5.5 Densification in Modern Networks

In the last section, we described different factors that affect how network performance scales with density and observed their individual impact. In modern networks, many of these factors simultaneously impact the system performance because of which their interplay will decide the asymptotic behavior, which may depart from the scaling performance studied for each factor separately in the previous section. To understand this, let us take a simple example. We observed that a non-zero height difference between the BS and UE could result in zero coverage probability as the network is densified. We also observed that coverage can increase to 1 by densification if the UE density is finite. Clearly, these two factors counter each other, and their cumulative effect depends upon the operational scenarios. This also makes it interesting to investigate the scaling behavior of a network with non-zero height difference and finite UE density, which we do next. For simplicity, we assume the single slope model. Initially, when density is low, the distances along the ground between the typical UE and different BSs will be large compared to the height difference because of which the height can be ignored. When the BS density increases, the SIR remains invariant. As BS density becomes of the order of the UE density, many BSs will start to go in the idle mode (because they do not have any UEs to serve). This reduces the sum interference which increases the SIR coverage probability. At further densification, the number of active BSs becomes constant at λ_u, and hence the potential throughput approaches a constant.

As the BS density approaches ∞, the height difference between the BS and the UE starts showing its effect. In particular, each UE has its serving BS right next to it because of which the serving power approaches a constant value given the lower bound on the path-loss. In addition, since the UE density is finite, the interference statistics would not change with BS densification after BS density gets high enough. This is because each active interfering BS will be located right next to the UE it is serving, and therefore, the point process of the interfering BSs will converge to the point process of the UEs (excluding of course the typical UE). Therefore, the SIR distribution becomes invariant to any further densification. This is contrary to the behavior with finite UE density and zero height difference where SIR coverage probability increases to 1 or under non-zero height difference with infinite UE density where the SIR coverage probability decreases to 0. The potential throughput also remains constant owing to the fact that both the SIR coverage and the active BS density are fixed.

The above discussion necessitates the study involving the interplay of all the factors to understand the exact behavior of a cellular network's performance under densification. In this section, we will consider some case studies where two or more than two factors are considered together.

5.5.1 Finite UE Density Under Multi-slope Path-Loss

We saw that under the single slope path-loss ($\alpha > 2$), with finite UE density, the coverage probability approaches 1. On the other hand, under the multi-slope path-loss with infinite UE density, the coverage probability approaches a constant (may go to zero if $\alpha_0 < 2$). Similarly, for the first case, the potential throughput approaches the constant value, whereas for the second case, the potential throughput increases linearly if $\alpha_0 > 2$, sublinearly if $1 \leq \alpha_0 < 2$ or even go to zero if $\alpha_0 < 1$.

When the UE density is finite, we observe a hybrid behavior under multi-slope path-loss model, as shown in the Fig. 5.13. With densification, the SIR coverage probability first decreases as interference from the BSs inside the corner distance becomes dominant. After the BS density supersedes the UE density, the interference remains bounded, while the serving power increases. This results in coverage probability becoming 1. The potential throughput, therefore, also increases as $\mathrm{p_c}$ increases, and then it approaches $\lambda_\mathrm{u} \log(1 + \gamma_\mathrm{s})$ asymptotically. This indicates that the densification beyond a point is not beneficial as the throughput gets saturated. Similar behavior is also observed for probabilistic two regime models and the two 3GPP models discussed earlier in the chapter [38].

5.5.2 Height Difference Between BS and UE Under Multi-slope Path-Loss

Figure 5.14 shows the behavior of network's performance under multi-slope path-loss when there is difference between the heights of the BS and UE antennas. We observe that height difference can result in a severe coverage and throughput crash.

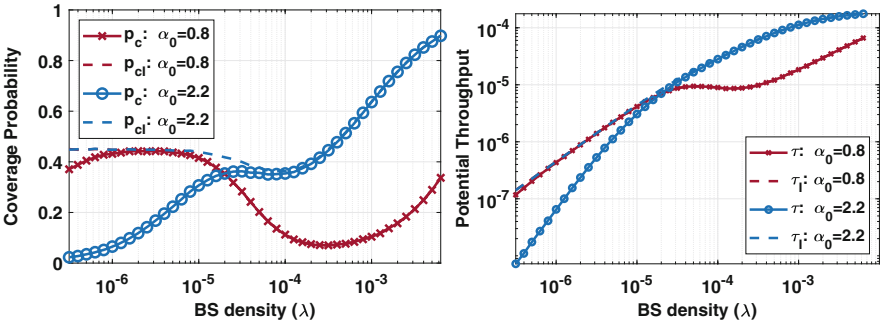

Fig. 5.13 Scaling of the coverage probability and potential throughput under multi-slope path-loss model when the UE density is fixed at 200 UE/km^2. Here, the path-loss model is taken as the dual-slope path-loss with $R_c = 100$ m, $C_0 = 10^{-7}$, $\alpha_0 = 0.8, 2.2$ and $\alpha_1 = 3.3$. $\gamma_\mathrm{s} = 1$. Dashed lines represent respective metrics in the absence of noise

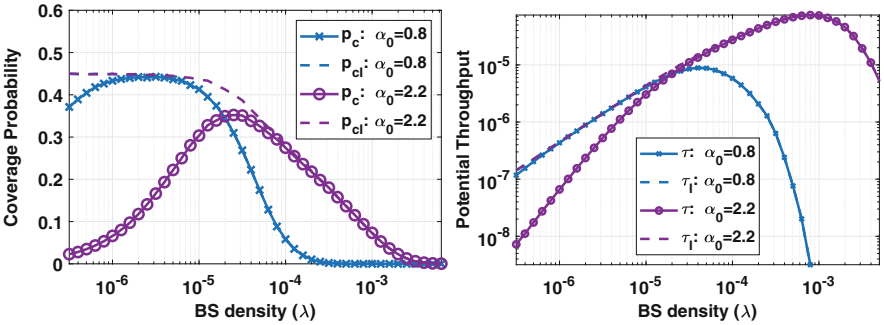

Fig. 5.14 Scaling of the coverage probability and potential throughput under multi-slope path-loss model when there is a height difference of $H = 10$ m between the BS and UE antennas. Here, the path-loss model is taken as the dual-slope path-loss with $R_c = 100$ m, $C_0 = 10^{-7}$, $\alpha_0 = 0.8, 2.2$, and $\alpha_1 = 3.3$. $\gamma_s = 1$. Dashed lines represent respective metrics in the absence of noise

Similar behavior is also seen under the probabilistic path-loss model, such as the 3GPP-Model-1 [39, 40].

5.5.3 *Fixed UE Density with Non-zero Height Difference Under Multi-slope and Probabilistic Path-Loss*

A network with fixed UE density and non-zero height difference between BSs and UE was studied in [41] under the probabilistic path-loss model, namely, 3GPP-Model-2. When the BS density is increased, SIR coverage $\mathrm{p_{cI}}$ first increases as the serving BS will be LOS with an increasing probability. Then at further densification, $\mathrm{p_{cI}}$ decreases as interferers start becoming LOS. As the BS density approaches the UE density, many of the BSs will be inactive, and this puts an upper bound on the interference. The serving power, however, increases with the BS density. Therefore, $\mathrm{p_{cI}}$ increases again. When we further densify, after a certain density λ', the serving power gets bounded owing to the fact that the serving BS distance cannot be smaller than the height difference H. The total interference is already bounded. This leads to a constant SIR coverage which may not be 1 and will be invariant of the further densification. The SINR decreases due to the non-zero BS-to-UE antenna height difference H, while it increases due to the BS idleness. This means that the two effects counterbalance each other to some extent. As the active BS density is also bounded, the potential throughput also becomes constant after a certain BS density λ'. Any network densification beyond such a level of BS density is a waste of both money and energy.

Note that in the above discussion, the UE density is finite. If the UE density is infinite (or if it scales with the BS density), the network capacity crashes as discussed before. However, this crash can be avoided if the number of active BSs

can be bounded. Instead of serving all users, a fraction of users can be served which will limit the total number of active BSs and hence the interference. This will lead to the similar asymptotic behavior as observed with the finite UE density.

5.5.4 *Access Restrictions with Finite UE Density*

We now consider a HetNet with two tiers and a finite UE density. Since there are two tiers, we assume that there are equal number of UEs subscribed to each tier. Our aim here is to evaluate the impact of access restriction on coverage and throughput of two tiers. In open access, UEs can connect to any network. Depending on the actual number of UEs associated with each tier, we evaluate the active BS density of that tier. In closed access, the UE can only connect to their own tier; therefore active density of BSs will depend on their UE density only. We first consider the case where both tiers densify equally. The results are shown in Fig. 5.15. For both open and closed access, coverage and throughput follow the same trend as observed in the single tier case with finite UE density. However, as also discussed earlier, closed access can reduce the coverage compared to the open access.

In asymmetric networks where one tier has higher density than the other, closed access can severely affect the performance of the latter network. The results are shown in Fig. 5.16. We consider that the first-tier density is fixed while the second tier densifies. The coverage in open access increases to 1 with densification of the second tier. This is due to the fact that densification of the second tier will cause most UEs to associate with the second tier. The first tier will only get those UEs which have better serving power from the first tier than the potential serving power of the highly dense second tier. The interference on the other hand remains bounded due to the limit on the total number of active BSs.

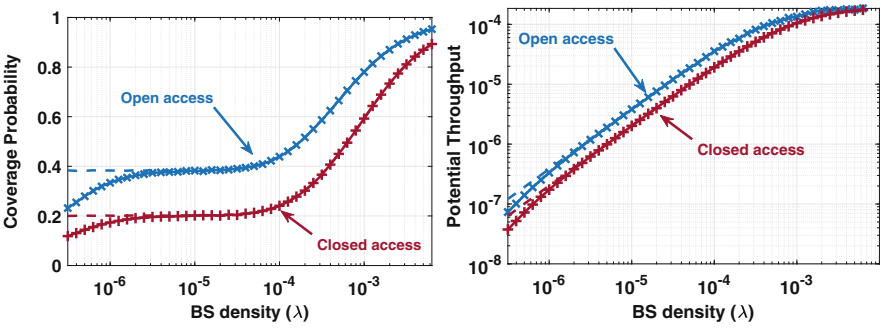

Fig. 5.15 Impact of densification under open and closed access for a two-tier network with the equal scaling of BS density for both tiers ($\mu_1 = \mu_2 = \lambda$) and fixed UE density 200 UE/km^2. The path-loss model is taken as the single slope path-loss with $C = 10^{-4}$ and $\alpha = 3$. Here, $\gamma_s = 1$. Dashed lines represent respective metrics in the absence of noise

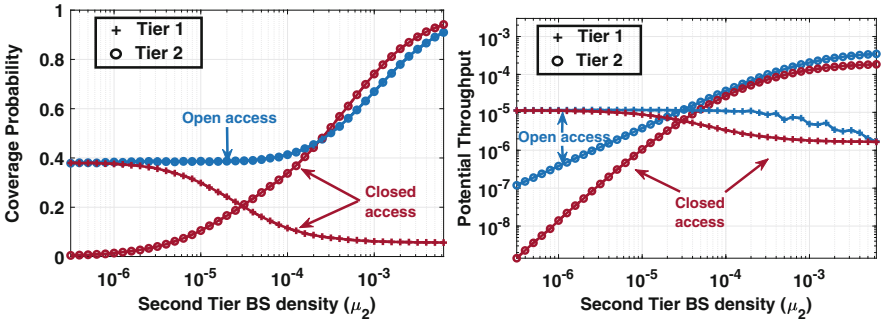

Fig. 5.16 Impact of the BS densification of the second tier on the coverage probability and potential throughput of the first tier in a two-tier asymmetric cellular network with different access restrictions. First tier has the fixed density $\mu_1 = 30\text{BS/km}^2$, while the second tier's BS density (μ_2) is varied. The path-loss model is taken as the single slope path-loss with $C = 10^{-4}$ and $\alpha = 3$. Here, $\gamma_s = 1$

Under closed access, the densification of the second tier drastically decreases coverage probability of the first tier. This is due to the fact that densification of the second tier will increase the interference, while the serving power depends on the first tier's BS density which is fixed. However, the coverage probability of the second tier increases with its densification.

The potential throughput of the first tier goes to zero in open access owing to the fact that the number of UEs associating with the first tier decreases. The potential throughput of the first tier also falls to zero in the closed access, but its fall is earlier than the one observed in open-access scenario, and it saturates afterward. However, the throughput of the second tier linearly increases with densification before saturating in the end, for both access mechanisms.

5.6 Conclusions

Having provided a comprehensive account of the densification gains in a variety of operational scenarios, we get back to the question that we asked early in the chapter: *Is densification the key to the future gains in cellular networks?*. As is the case with many questions in practice, unfortunately, the answer is: *it depends*. In particular, we have seen that while densification helps in many scenarios, it can also cause the SINR and throughput crash in some other scenarios. There are far many important factors that affect the conclusion significantly and may result in drastically different scaling results. Some of these major factors are the path-loss models, the height difference, and scaling of the UE density with the BS density. At the same time, some factors, such as the fading distribution and directionality,

may not have as drastic of an impact on the eventual conclusions, especially for the asymptotic results. In practical systems, many of these factors impact system performance simultaneously because of which it is important to understand the interplay between these factors and how they jointly impact the performance. In order to provide key insights about these interplays, we included some important case studies in which two or more such factors were considered jointly. However, the eventual conclusions on the scaling of the network performance still remains highly dependent on the system configuration. This again highlights the importance of using accurate models and operational regimes for the performance analysis of cellular networks.

References

1. Cisco Systems Inc., Cisco visual networking index: global mobile data traffic forecast update, 2015–2020. Growth Lakel. **2011**(4), 2010–2015 (2011)
2. Ericsson, Ericsson mobility report, Nov 2019, accessed: 2020-04-20. [Online]. Available: https://www.ericsson.com/4acd7e/assets/local/mobility-report/documents/2019/emr-november-2019.pdf
3. Arraycomm, Cooper's Law. [Online]. Available: http://www.arraycomm.com/technology/coopers-law
4. N. Bhushan, J. Li, D. Malladi, R. Gilmore, D. Brenner, A. Damnjanovic, R.T. Sukhavasi, C. Patel, S. Geirhofer, Network densification: the dominant theme for wireless evolution into 5G. IEEE Commun. Mag. **52**(2), 82–89 (2014)
5. J.G. Andrews, X. Zhang, G.D. Durgin, A.K. Gupta, Are we approaching the fundamental limits of wireless network densification? IEEE Commun. Mag. **54**(10), 184–190 (2016)
6. X. Ge, S. Tu, G. Mao, C.X. Wang, T. Han, 5G Ultra-Dense Cellular Networks. IEEE Wirel. Commun. **23**(1), 72–79 (2016)
7. M. Ding, D. López-Pérez, H. Claussen, M.A. Kaafar, On the fundamental characteristics of ultra-dense small cell networks. IEEE Netw. **32**(3), 92–100 (2018)
8. A.K. Gupta, A. Alkhateeb, J.G. Andrews, R.W. Heath, Gains of restricted secondary licensing in millimeter wave cellular systems. IEEE J. Sel. Areas Commun. **34**(11), 2935–2950 (2016)
9. J.G. Andrews, F. Baccelli, R.K. Ganti, A tractable approach to coverage and rate in cellular networks. IEEE Trans. Commun. **59**(11), 3122–3134 (2011)
10. J.G. Andrews, A.K. Gupta, H.S. Dhillon, A primer on cellular network analysis using stochastic geometry, arXiv preprint arXiv:1604.03183, 2016
11. A. Guo, M. Haenggi, Asymptotic deployment gain: a simple approach to characterize the sinr distribution in general cellular networks. IEEE Trans. Commun. **63**(3), 962–976 (2015)
12. R.K. Ganti, M. Haenggi, Asymptotics and approximation of the SIR distribution in general cellular networks. IEEE Trans. Wirel. Commun. **15**(3), 2130–2143 (2016)
13. H.P. Keeler, N. Ross, A. Xia, When do wireless network signals appear poisson? arXiv preprint arXiv:1411.3757, 2014
14. N. Ross, D. Schuhmacher, Wireless network signals with moderately correlated shadowing still appear poisson. IEEE Trans. Inf. Theory **63**(2), 1177–1198 (2017)
15. H.S. Dhillon, M. Kountouris, J.G. Andrews, Downlink MIMO HetNets: modeling, ordering results and performance analysis. IEEE Trans. Wireless Commun. **12**(10), 5208–5222, (2013)
16. B. Blaszczyszyn, M.K. Karray, Spatial Distribution of the SINR in Poisson Cellular Networks With Sector Antennas. IEEE Trans. Wirel. Commun. **15**(1), 581–593 (2016)

17. H.S. Dhillon, R.K. Ganti, F. Baccelli, J.G. Andrews, Modeling and analysis of K-tier downlink heterogeneous cellular networks. IEEE J. Sel. Areas Commun. **30**(3), 550–560 (2012)
18. X. Zhang, J.G. Andrews, Downlink cellular network analysis with multi-slope path loss models. IEEE Trans. Commun. **63**(5), 1881–1894 (2015)
19. T. Bai, R.W. Heath Jr., Coverage and rate analysis for millimeter wave cellular networks. IEEE Trans. Wirel. Commun. **14**(2), 1100–1114 (2015)
20. Y. Wu, P. Butovitsch, M. Zhang, Capacity upper bound for adding cells in the super dense cellular deployment scenario, in *Proceedings of the IEEE Vehicular Technology Conference (VTC Spring)*, May 2014, pp. 1–5
21. X. Zhang, J.G. Andrews, Downlink cellular network analysis with a dual-slope path loss model, in *Proceedings of the IEEE International Conference on Communication (ICC)*, vol. 2015, Sept 2015, pp. 3975–3980
22. A.K. Gupta, J.G. Andrews, R.W. Heath, On the feasibility of sharing spectrum licenses in mmWave cellular systems. IEEE Trans. Commun. **64**(9), 3981–3995 (2016)
23. M.N. Kulkarni, E. Visotsky, J.G. Andrews, Correction factor for analysis of mimo wireless networks with highly directional beamforming. IEEE Wireless Commun. Lett. **7**(5), 756–759 (2018)
24. M. Ding, D. Lopez-Perez, G. Mao, P. Wang, Z. Lin, Will the area spectral efficiency monotonically grow as small cells go dense?, in *Proceedings of the IEEE GLOBECOM*, 2015
25. M. Ding, P. Wang, D. López-Pérez, G. Mao, Z. Lin, Performance impact of LoS and NLoS transmissions in dense cellular networks. IEEE Trans. Wirel. Commun. **15**(3), 2365–2380 (2016)
26. 3GPP, 3GPP TR 36.828 (V11. 0.0): further enhancements to LTE Time Division Duplex (TDD) for Downlink-Uplink (DL-UL) interference management and traffic adaptation, Tech. Rep., 2012
27. AHG, Spatial Channel Model, Subsection 3.5. 3, Spatial Channel Model Text Description V6. 0, Tech. Rep., 2003
28. S. Singh, H.S. Dhillon, J.G. Andrews, Offloading in heterogeneous networks: modeling, analysis and design insights. IEEE Trans. Wirel. Commun. **12**(5), 2484–2497 (2013)
29. A.K. Gupta, X. Zhang, J.G. Andrews, Potential throughput in 3D ultradense cellular networks, in *Proceedings of the Asilomar Conference on Signals, System and Computers*, Nov. 2015, pp. 1026–1030
30. D. López-Pérez, M. Ding, H. Claussen, A.H. Jafari, Towards 1 Gbps/UE in cellular systems: understanding ultra-dense small cell deployments. IEEE Commun. Sur. Tutorials **17**(4), 2078–2101 (2015)
31. A.K. Gupta, M.N. Kulkarni, E. Visotsky, F.W. Vook, A. Ghosh, J.G. Andrews, R.W. Heath, Rate analysis and feasibility of dynamic TDD in 5G cellular systems, in *Proceedings of the IEEE International Conference on Communications (ICC)*, May 2016, pp. 1–6
32. J.G. Andrews, T. Bai, M.N. Kulkarni, A. Alkhateeb, A.K. Gupta, R.W. Heath, Modeling and analyzing millimeter wave cellular systems. IEEE Trans. Commun. **65**(1), 403–430 (2017)
33. V.V. Chetlur, H.S. Dhillon, Downlink coverage analysis for a finite 3-D wireless network of unmanned aerial vehicles. IEEE Trans. Commun. **65**(10), 4543–4558 (2017)
34. A.K. Gupta, X. Zhang, J.G. Andrews, SINR and throughput scaling in ultradense urban cellular networks. IEEE Wireless Commun. Lett. **4**(6), 605–608 (2015)
35. A. Merwaday, R. Vannithamby, M.M. Rashid, Z. Yi, C. Clark, X. Wu, On the performance of directional communications in ultra-dense networks, in *Proceedings of the IEEE International Conference on Communication (ICC) Workshop*, 2017, pp. 522–527
36. A.K. Gupta, H.S. Dhillon, S. Vishwanath, J.G. Andrews, Downlink multi-antenna heterogeneous cellular network with load balancing. IEEE Trans. Commun. **62**, 4052–4067 (2014)
37. A.K. Gupta, Asymmetric multi-tier dense networks with access restrictions, 2020, accessed: 2020-04-20. [Online]. Available: http://home.iitk.ac.in/~gkrabhi/asymmtaccess/
38. M. Ding, D. Lopez Perez, G. Mao, Z. Lin, Study on the idle mode capability with LoS and NLoS transmissions, in *Proceedings of the IEEE GLOBECOM*, 2016

39. M. Ding, D.L. Perez, Please lower small cell antenna heights in 5G, in *Proceedings of the IEEE GLOBECOM*, 2016, pp. 1–6
40. M. Ding, D. López-Pérez, Performance impact of base station antenna heights in dense cellular networks. IEEE Trans. Wirel. Commun. **16**(12), 8147–8161 (2017)
41. M. Ding, D. López-Pérez, G. Mao, Z. Lin, Ultra-dense networks: is there a limit to spatial spectrum reuse?, in *Proceedings of the IEEE International Conference on Communication (ICC)*, 2018, pp. 1–6